Surface alloying of indium on Cu(111)

2003 J. Phys.: Condens. Matter 15 1909

(http://iopscience.iop.org/0953-8984/15/12/308)

INSTITUTE OF PHYSICS PUBLISHING JOURNAL OF PHYSICS: CONDENSED MATTER

J. Phys.: Condens. Matter **15** (2003) 1909–1919 PII: S0953-8984(03)52819-3

Surface alloying of indium on Cu(111)

H Wider[1], V Gimple[1], W Evenson[1,3], G Schatz[1], J Jaworski[2], J Prokop[2] and M Marszałek[2]

[1] Department of Physics, University of Konstanz, D-78457 Konstanz, Germany
[2] The H Niewodniczański Institute of Nuclear Physics, Kraków, Poland

Received 29 August 2002, in final form 10 February 2003
Published 17 March 2003
Online at stacks.iop.org/JPhysCM/15/1909

Abstract

An ultrathin film of indium deposited on Cu(111) has been studied by an *in situ* combination of medium-electron energy diffraction, low-energy electron diffraction, scanning tunnelling microscopy and Auger electron spectroscopy. The surface alloys, Cu_2In and Cu_3In, which do not exist in these structures in the bulk, have been found in this system.

1. Introduction

New and unusual alloy phases, not existing in the bulk, are known to form at surfaces and interfaces as well as in nanostructures. For example, as early as 1985, the surprising alloy $CuIn_2$ was found at Cu–In thin-film interfaces [1]. Lowering the dimensionality leads to interface alloy formation with possibly unexpected properties and structures. Typically, the stability range of such low-dimensional structures differs substantially from that of bulk materials [2]. The study of such unusual alloy phases is of practical importance for the magnetic, electrical and mechanical properties of thin-film and nanostructured systems as well as being of fundamental interest for understanding metal–metal interactions at surfaces, in thin films and in nanostructures. Indium, in particular, is important in such studies since it acts as a surfactant for the deposition of films of other metals. Surfactants modify interactions at surfaces to facilitate layer-by-layer growth, while continually segregating to the surface. Surfactants are especially important in the preparation of many layered materials. An example of the surfactant effect of indium is that it assists copper to grow smooth Cu(111) films on a substrate, instead of islands and clumps [3]. Also, because indium atoms are much larger than copper ($r_{In} = 0.167$ nm, $r_{Cu} = 0.128$ nm), not unlike the relation of antimony to copper ($r_{Sb} = 0.159$ nm), the details of indium interactions with copper at surfaces are interesting in themselves: how do dissolution and segregation take place when these large atoms are deposited on the close-packed Cu(111) surface? This work investigates the formation of new metastable intermetallic phases created in the deposition of indium on the Cu(111) surface.

[3] Permanent address: Department of Physics and Astronomy, Brigham Young University, Provo, UT 84602, USA.

0953-8984/03/121909+11$30.00

While these phases appear at surfaces and interfaces, they are not known in the same structure from the bulk phase diagram at room temperature.

It is known from perturbed angular correlation (PAC) experiments that, in spite of the large size mismatch, the equilibrium position of isolated indium on Cu(111) is in substitutional terrace sites, and further, that In–In interactions in such contexts are attractive, so indium forms pairs or clusters [4]. Available evidence suggests that, due to the large relative size of the indium atoms, pairs or clusters form at second-neighbour positions, so each indium remains surrounded by copper atoms. Theoretical calculations of van Siclen [5] for the Cu(111) and (001) surfaces indicate that second-neighbour pairs are energetically favoured over nearest-neighbour pairs, similar to results of Breeman *et al* [6] for the Cu(100) surface. As discussed more fully below, experimental data of Klas *et al* [4], Breeman and co-workers [7–9] and van Gastel and co-workers [10, 11] can all be interpreted to indicate that indium pairs or clusters form with indium atoms in relative second-neighbour positions.

Because of its interest as a surfactant, antimony on Cu(111) and on Ag(111) has also been studied extensively [12–14]. With antimony one finds a surface structure giving a $p(\sqrt{3} \times \sqrt{3})R30°$ surface reconstruction on both Cu(111) and Ag(111) at low coverage (1/3 to 1/2 ML Sb) ([14], and references therein). At higher coverages, a $p(2\sqrt{3} \times 2\sqrt{3})R30°$ reconstruction has been observed on Ag(111), and explained as 'an ordered $p(2 \times 2)$-Sb overlayer superimposed on the $(\sqrt{3} \times \sqrt{3})R30°$-Sb surface' [12]. In the Sb–Cu(111) system the atomic structure of the CuSb surface alloy has been determined to be the substitutional alloy Cu_2Sb [15, 16]. Theoretical calculations have also shown that the creation of this surface alloy is energetically favoured [17]. These results for Sb–Cu and the similarities between the Sb–Cu and In–Cu systems (surface free energies of metals, sizes of atoms) serve as a reference point for studies of the growth of indium on the Cu(111) surface.

The atomic structure of an ultrathin layer of indium on Cu(111) was investigated in the present work by an *in situ* combination of medium-electron energy diffraction (MEED), low-energy electron diffraction (LEED), scanning tunnelling microscopy (STM) and Auger electron spectroscopy (AES).

2. Experimental details

Sample preparation and characterization were done in an ultrahigh-vacuum system at pressures below 10^{-8} Pa. Copper single crystals were prepared from a (111)-oriented rod that was polished mechanically and electrochemically. The Cu(111) surface was cleaned in ultrahigh vacuum by alternate cycles of argon ion sputtering (argon energy 250–760 eV) and annealing at 600 °C for times ranging from 5 min to 1 h/cycle. Indium films were deposited at rates between 0.05 and 0.5 ML min^{-1} by thermal evaporation at a working pressure in the range of 10^{-8} Pa. Indium film thickness was controlled during evaporation with a quartz thickness monitor, and MLs were defined to be equivalent MLs of pure indium layers with the bulk lattice constant. During deposition the sample was kept at room temperature.

At each step the sample surface was checked *in situ* by AES and never showed residual gas contamination greater than 0.01 ML. Peak-to-peak AES intensities were measured during deposition of indium for the 60 and 920 eV Cu lines and for the 404 eV In line.

The growth of the film was monitored *in situ* by MEED (2.7 keV). MEED intensity measurements were taken from windows positioned at various points on specular and superstructure reflections. Relative lattice constant changes were measured by accurate line scans showing spot separations during deposition of indium.

In situ LEED and STM measurements were not possible in our experimental set-up. Therefore, after deposition the samples were transferred into different positions in the chamber,

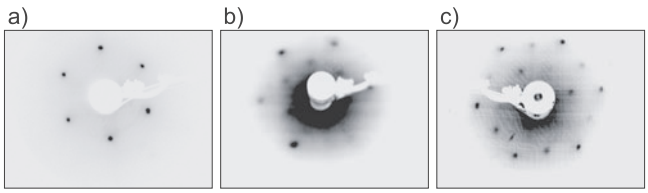

Figure 1. LEED patterns for the Cu(111) surface: (a) bare copper surface, (b) with nominal 0.5 ML indium deposited and (c) with nominal 1.0 ML indium deposited. Sample orientations were rotated a little between measurements, and the pictures were taken at slightly different electron energies.

and the surface was analysed. LEED images were observed for various electron energies to provide information as a function of depth. We used a commercial STM from RHK, Inc. that operates at variable temperatures from 100 to 500 K.

3. Results

A sequence of LEED patterns obtained during room-temperature deposition of indium is shown in figure 1. The image of the bare copper surface shows a typical pattern characteristic of a well ordered (111) surface. Upon initial indium deposition, the p(1 × 1) diffraction spots of the clean surface became dimmer, and near 0.5 ML of deposited indium we observed a pattern corresponding to a well ordered surface with a p($\sqrt{3} \times \sqrt{3}$)R30° reconstruction. The p($\sqrt{3} \times \sqrt{3}$)R30° reconstruction was only observed at electron energies between 102 and 142 eV, but the unreconstructed copper surface pattern was observed at higher energies.

Depositing additional indium to near 0.8 ML resulted in a change of this pattern to a p(2 × 2) reconstruction, which was seen up to about 1.5 ML. Increasing LEED electron energy up to 400 eV did not influence the p(2 × 2) image, suggesting that this reconstruction persists into deeper layers below the surface. With additional indium deposition, the p(2 × 2) pattern disappeared, and the LEED image showed only the diffuse scattering background.

The MEED specular beam intensity was observed during indium deposition. Pronounced variations occurred in this intensity, with maxima near 0.5 ML and a little before 1 ML of indium, as shown in figure 2(a). During observation of the specular beam intensity, additional spots appeared, corresponding to the reconstructed surface. We have also measured the evolution of the intensities of these superstructure spots. MEED intensities of the spots corresponding to both surface reconstructions were measured simultaneously during indium evaporation, as shown in figures 2(b) and (c).

The conversion of the p($\sqrt{3} \times \sqrt{3}$)R30° reconstructed surface into the p(2 × 2) reconstruction at higher indium coverages is seen clearly in the two MEED intensity maxima. The MEED intensity of the spot related to the p($\sqrt{3} \times \sqrt{3}$)R30° reconstruction, shown in figure 2(b), reached its maximum at about 0.45 ML of indium coverage, and then the intensity fell back toward the diffusive background intensity. At this same coverage, the intensity of the p(2 × 2) spot changed very little, and only began to increase around 0.7 ML of indium, with maximum slightly below 1 ML, as shown in figure 2(c). This spot intensity then decreased slowly to background, reaching that level at about 5 MLs of indium.

The relative lattice expansion due to indium incorporation is shown in figure 3, as measured by MEED during deposition of indium. The electron beam was oriented along the azimuthal direction ⟨1, 1, −2⟩ of the sample and the separation of the (2, −2, 0) and (−2, 2, 0) MEED spots was analysed. These data show that the surface lattice constant, normalized to the pure copper surface lattice constant, increased and reached a saturation of about 15% at an indium

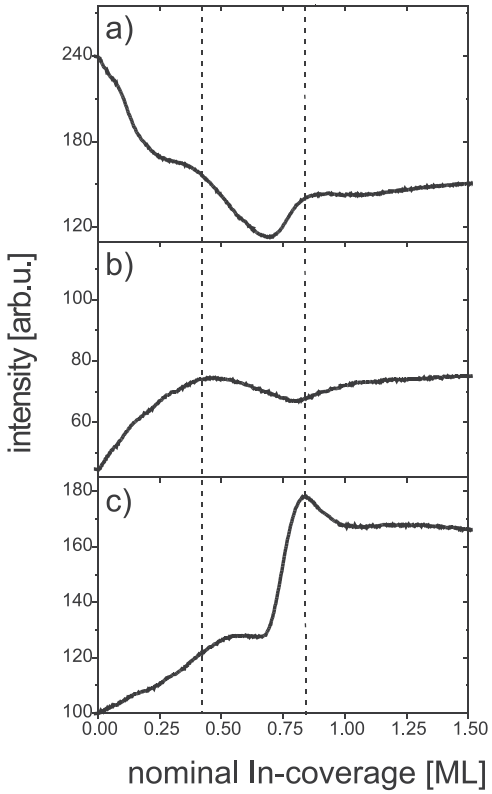

Figure 2. MEED intensities: (a) specular intensity during evaporation of indium onto Cu(111), (b) p($\sqrt{3} \times \sqrt{3}$)R30° superstructure reflection intensity (intensity beyond the dip at 0.8 ML is at background) and (c) p(2 × 2) superstructure reflection intensity (intensity before 0.7 ML is at background).

coverage of about 0.4 ML. At higher coverages, where the Cu_3In alloy is formed, no further changes in lattice parameters are observed within experimental error.

AES measurements are shown in figures 4 and 5. Peak-to-peak intensities, measured during the deposition of indium for 404 eV In Auger electrons (figure 4), increased with indium coverage to the coverage at which the surface layer was completed. Further indium deposition resulted in a small region of slower increase, followed by a renewed intensity increase. In figure 5 we see peak-to-peak intensities for two copper lines, Cu_{MNN} at 60 eV and Cu_{LMM} at 920 eV during indium deposition. The low-energy line, with smaller electron penetration depth, decays significantly more quickly than the high-energy line. Reliable determination of the Cu–In stoichiometry is not possible since there is always a strong contribution from the underlying copper substrate, due to the penetration depth of the electron beam.

STM images of the surface development at successive stages of indium deposition in the low-coverage range, together with a height distribution histogram, are shown in figure 6. The histogram is simply a plot of pixel heights from representative windows in the image. Note that these STM images show microscopic local topography, while LEED, MEED and AES provide information on macroscopic structure on the scale of the beam size. The bare copper surface exhibits only large, flat terraces of different heights. Deposition of 0.125 ML indium results in irregularly shaped agglomerates, randomly positioned on the terraces, and not attached to the

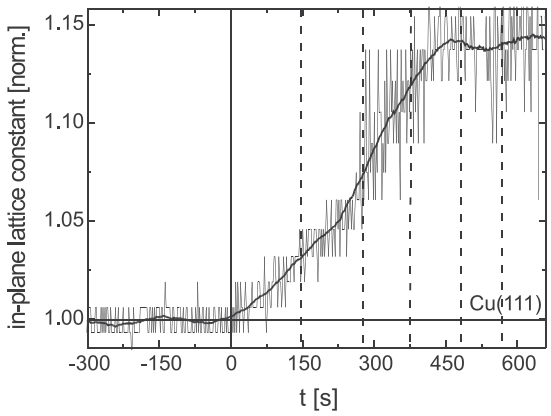

Figure 3. Surface lattice constant for the Cu_2In surface layer relative to Cu(111), showing approximately 15% expansion at about 0.5 ML indium. Dotted vertical lines are shown at about 1/8 ML intervals.

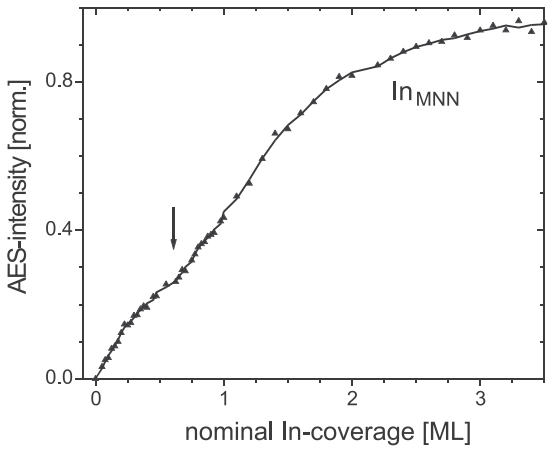

Figure 4. Auger peak-to-peak intensity of the In_{MNN} (404 eV) signal, normalized to the high-coverage value. The line is a guide for the eye.

terrace steps. Increasing indium coverage leads to increased island density. In some areas a second layer could be seen. The holes in the islands observed mainly at lower indium coverage are probably vacancy clusters, helping release the surface stress induced by the large indium atoms.

At 0.5 ML indium the islands nearly fill the terraces, so only the terrace steps are evident. The height distribution histogram shows a small peak between two terrace positions at height 0.161 nm, corresponding to the alloy on the surface.

At 1 ML of coverage (figure 7) the agglomerates vanish, and the surface is covered by completely closed layers. However, the step shape has changed to a much more irregular structure. The steps on the surface are of varying heights, mostly single and double layers. At 5–6 MLs three-dimensional growth of indium was observed.

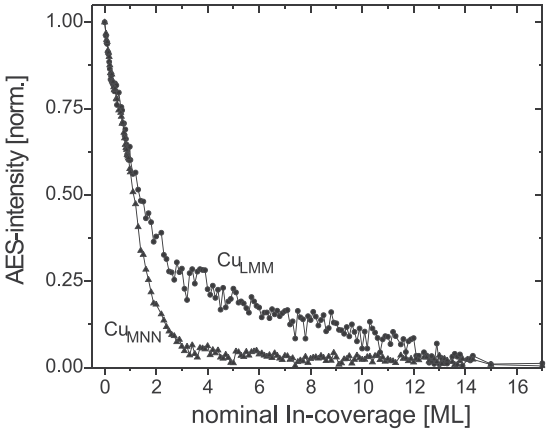

Figure 5. Auger peak-to-peak intensity of the Cu_{LMM} (920 eV) and Cu_{MNN} (60 eV) signals, normalized to the high-coverage value.

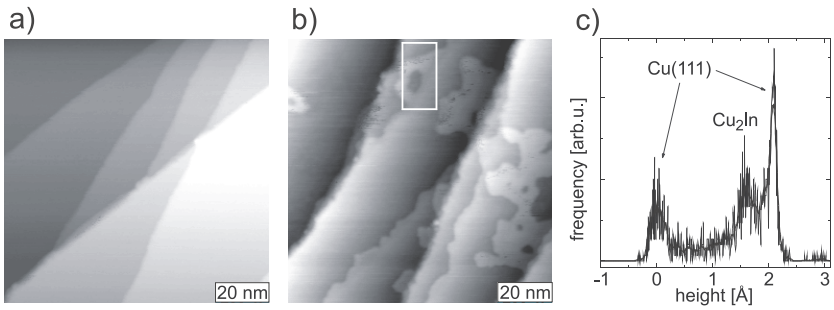

Figure 6. STM images showing (a) clean copper surface with steps and (b) nominal 0.1 ML indium coverage. (c) Height histogram taken from the window shown in (b). The bar at the lower right of each image is 20 nm in length.

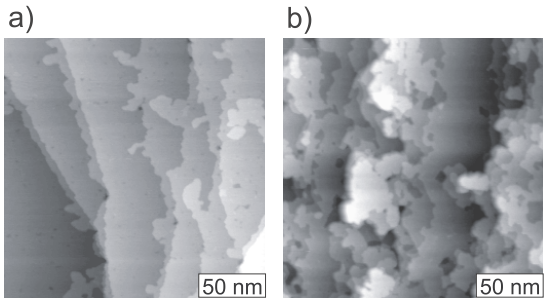

Figure 7. STM images of surface with nominal (a) 1 ML and (b) 2.5 ML indium coverage. The bar at the lower right of each image is 50 nm in length.

4. Cu_2In ($\leqslant$0.5 ML indium)

The LEED pattern taken with 0.5 ML indium deposited on Cu(111) showed a well ordered surface with p($\sqrt{3} \times \sqrt{3}$)R30° reconstruction for low energies (102–142 eV). This suggests that the surface is now covered with a new well ordered phase and that this phase is only at or close to the surface, since the reconstruction was observed only for low LEED energies

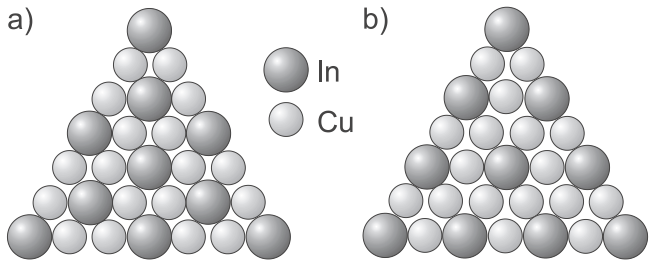

Figure 8. Schematic representation of (a) the p($\sqrt{3} \times \sqrt{3}$)R30° and (b) the p(2 × 2) real space structures.

(corresponding to electron penetration depth of 0.28–0.33 nm [18]). This interpretation of the LEED data is also consistent with the stoichiometry of the alloy and the geometrical coverage of this alloy as determined below.

The MEED specular reflection intensity showed a maximum near 0.5 ML, and at approximately the same point (0.4–0.5 ML) the intensity of the p($\sqrt{3} \times \sqrt{3}$)R30° superstructure spot reached a maximum. These maxima suggest that the new surface layer is completed and that additional indium deposition no longer increases the p($\sqrt{3} \times \sqrt{3}$)R30° phase. In fact, as stated above, the LEED pattern begins to change at that point.

The MEED and LEED observations are consistent: the sub-monolayer maxima of the specular beam and superstructure spot intensities indicate successive filling of the surface layer with the addition of indium. The appearance of the maxima is strongly correlated with the appearance of the surface reconstructions and can be interpreted as a creation of a new ordered surface phase.

Knowing the amount of indium deposited, and bearing in mind that the p($\sqrt{3} \times \sqrt{3}$)R30° ordered surface phase corresponds to 2:1 stoichiometry [13], we conclude that the intermixed topmost layer is an ordered surface alloy of composition Cu_2In. Then indium atoms would substitute for one-third of the copper atoms in the surface layer and form a single-layer surface alloy phase, as indicated by our LEED patterns. Figure 8(a) shows the schematic presentation of the real-space atomic positions on the surface for the reconstructed alloy.

The most important question for understanding surface alloying or surface mixing is to deduce the adatom positions in the newly created surface superstructure. Therefore, it seems worthwhile to look carefully at the arguments leading to the assignment of the Cu_2In surface alloy phase, as well as reviewing our additional data. Usually one has to consider at least two possibilities, an overlayer of adatoms sitting on the host lattice sites and substitutional surface positions of adatoms leading to the formation of the surface alloy. From earlier perturbed $\gamma\gamma$-angular correlation (PAC) experiments [4, 19–22], it is known that at room temperature indium occupies only substitutional sites on Cu(111). The PAC data also show that indium forms clusters in the Cu(111) surface, and the very small shift of electric field gradients observed for these clusters [4] is highly suggestive that indium atoms are trapped at second-neighbour positions, as implied by theory [5, 6]. The work of van Gastel *et al* [10, 11] combined atomic resolution STM with PAC on Cu(100) to reach similar conclusions. The assignment of indium to substitutional sites in the copper surface, with each indium surrounded by copper, is consistent with the unit cell proposed in figure 8(a).

Low-energy ion scattering (LEIS) experiments performed to determine indium mobilities on a stepped Cu(100) surface have also shown that substitutional indium can be seen at temperatures as low as 100 K, and at room temperature all indium atoms occupy substitutional sites [7, 8]. Since surface diffusion activation energies for indium on Cu(100) and Cu(111)

are very similar [20], this observation provides additional support for the interpretation that indium also occupies substitutional sites in the Cu(111) surface below room temperature. LEIS has found that indium atoms in Cu(100) substitutional sites protrude from the surface by an amount consistent with the geometry of atoms of the respective sizes of indium and copper [7], which our STM height histograms also showed for Cu(111). These data and accompanying Monte Carlo calculations are also consistent with indium atoms preferentially in relative second-neighbour positions [6–8].

As shown in figure 3, the in-plane lattice constant for the p($\sqrt{3} \times \sqrt{3}$)R30° reconstruction is about 15% greater than that for Cu(111). A simple geometrical calculation using the nominal atomic radii and assuming that indium sits substitutionally in the surface finds an expected lattice expansion of 14.8%, in agreement with these observations. Hence these data also confirm the assignment of indium to substitutional surface positions. Furthermore, the fact that the observed expansion is just the geometrical value implies that this structure almost ideally releases the strain imposed by the larger indium atoms.

Finally, the conclusion that indium goes into substitutional surface positions is consistent with recent results [13–17] obtained for p($\sqrt{3} \times \sqrt{3}$)R30°-Sb reconstructions of Ag(111) and Cu(111) surfaces, also with a large atomic size mismatch. Moreover, the p($\sqrt{3} \times \sqrt{3}$)R30°-Sb reconstruction of the Ag and Cu surfaces is seen in dissolution and segregation kinetics studies, always leading to this reconstruction at 1/3 ML Sb. The fact that the alloy can be formed by either segregation or dissolution implies that this is an equilibrium structure. The out-of-plane displacement of antimony incorporated into the copper surface is also consistent with this picture of the larger antimony atoms substituting for copper. The antimony atoms protrude out of plane, whereas the copper atoms either remain in their original positions or relax into the plane [14, 16].

The similar alloying behaviour for indium in Cu(111) and antimony in Cu(111) and Ag(111) shows that, for at least several cases, when much larger atoms are deposited, they are not necessarily excluded by strain from the substrate but can be incorporated into it. We conclude that large atomic size mismatch does not, in general, impede surface alloy formation.

From the previous arguments, it seems likely that the islands seen in the STM images (figure 6) are Cu_2In alloy agglomerates. Estimating the height of the new agglomerate from the STM data, we find it at 0.161 nm above the lower terrace step, a value in agreement with that calculated by considering the high point of an indium hard sphere placed in a substitutional position in Cu(111).

These arguments as a whole, from our LEED, MEED, AES and STM data, from the earlier PAC and LEIS data, from theory and from the related antimony work, are all consistent in confirming the interpretation that the initial layer is an ordered Cu_2In surface alloy.

5. Cu_3In (>0.5 ML indium)

When more than 0.5 ML indium is deposited, both LEED and MEED show the formation of a new phase that penetrates deeper into the copper substrate. The p($\sqrt{3} \times \sqrt{3}$)R30° reconstruction changed to p(2 × 2). This new phase persisted up to between 1 and 2 ML and was seen for LEED energies up to 400 eV (electron penetration depth of 0.54 nm). In this range of indium deposition, the surface evidently consists of copper and indium intermixed through a significant depth.

The MEED specular reflection intensity showed a second maximum a little below 1 ML, indicating that the surface phase associated with the p(2 × 2) reconstruction has filled the surface at that point. The MEED intensity of the p(2 × 2) spot increased from 0.7 ML and reached a maximum at 0.8–0.9 ML.

The MEED and LEED observations are again consistent: now, with more indium deposited, we see the change from laying down a surface layer of Cu_2In to a new structure that penetrates deeper into the copper surface. The new structure gives rise to the p(2 × 2) reconstruction.

Looking first at the implications of the p(2 × 2) reconstruction for possible real-space arrangements of indium and copper in the new phase, we find possible structures corresponding to 3:1 or 1:3 stoichiometry. Knowing the amount of indium deposited, the size mismatch, and that the indium is distributed through at least two to three copper layers below the surface, we conclude that the new phase is an ordered surface alloy of composition Cu_3In. This composition, seen in schematic form in figure 8(b), also has a natural three-dimensional extension, i.e. layers of this alloy can be stacked while maintaining similar atomic surroundings. The arguments given above that indium enters the copper surface substitutionally and prefers to be surrounded by copper also apply here and support the proposed Cu_3In unit cell. It can easily be seen from the figure that the p(2 × 2) unit cell is consistent with Cu_3In stoichiometry for this alloy phase. This phase also extends several layers into the copper surface, producing several layers of the new alloy and implying considerable In/Cu interdiffusion, even at room temperature.

The stacking of this p(2 × 2) alloy in successive layers, implied by the geometry to be either cubic or hexagonal, was studied by LEED. As a function of increasing electron energy, the p(2 × 2) image alternated from threefold to sixfold symmetry, giving evidence of fcc-like stacking of planes[4]. This alternation of pattern symmetry is suggestive of a cubic structure for Cu_3In of type Cu_3Au ($L1_2$), which is not known in the bulk phase diagram. The assignment of cubic structure for Cu_3In is also consistent with the Hume-Rothery electron–atom ratio, which is 1.5 for Cu_3In, well below the 1.69 cut-off for hexagonal structures [23].

AES results can be related to the transition of the surface alloy from Cu_2In to Cu_3In (figure 4). Peak-to-peak intensities increased until completion of the Cu_2In layer, then slowed, with a short, relatively flat intensity, showing a dip in the progression of the intensity curve. The flatter section indicates that when additional indium is deposited, nearly as much as is deposited must be hidden to AES by being beyond the electron effective mean free path. There are two effects that could lead to this 'hidden' indium: piling up multiple layers of indium on the islands visible in the STM images, and diffusion of copper up into regions of excess indium. It is likely that both effects occur, as seen in the formation of the new alloy (Cu_3In). The AES intensities again increased once the transition process from Cu_2In to Cu_3In was completed, now due to additional indium being enriched at the surface.

These changing rates of AES intensity increase can be related to the large size mismatch between copper and indium: when the surface alloy can no longer accommodate more indium because of its large size, depositing additional indium leaves some indium initially in an overlayer and associates a large strain field with the indium that is incorporated into the copper–indium mixed interface layers. These strains are relieved by diffusion of more copper up into the mixed layers (and diffusion of indium down to deeper layers), forming a new alloy.

The copper AES results (figure 5) show clearly that after about 3 ML nominal indium coverage, the surface layer is indium rich, while a copper–indium intermixing is present for several layers below the surface. The low-energy signal, at 60 eV, incident at 77° from normal, has an effective electron mean penetration depth of 0.11 nm, while the high-energy signal, 920 eV, incident at 77°, has an effective mean penetration depth of 0.38 nm. The low-energy copper line essentially disappears by 3 ML indium, while the high-energy line persists until

[4] That fcc-like LEED patterns alternate between three- and sixfold symmetries with increasing depth, while hcp-like patterns maintain sixfold symmetry, can be seen easily by examining models of the respective reciprocal lattices (bcc and hexagonal). This pattern symmetry alternation is known quite generally among workers in the field.

about 12 ML indium. The two signals diverge from one another beginning at about 1 ML, with the high-energy line beginning an essentially linear descent at about 3 ML. Since only the top two layers contribute detectably to the low-energy signal, the Cu–In alloy is visible in the Cu_{MNN} signal up to about 3 ML of indium coverage. Then, with more indium coverage, the alloy containing copper is completely covered, suppressing this AES signal. However, the high-energy signal shows contributions from a depth of 4–5 ML. The region of linear decrease of this signal indicates clearly that copper diffuses toward the surface; otherwise, the signal would be exponentially absorbed. The pure indium signal is only seen at about 12 ML indium coverage, requiring copper diffusion into about the first 7 ML of indium deposition. These experiments did not investigate the kinetics of the diffusion and alloy formation process, so we cannot comment on whether the situation shown in figure 5 remains stable or whether additional copper diffusion occurs over time.

The morphology observed in the STM images (figure 7) is consistent with this picture, terraces being covered with indium, Cu_3In alloy and copper–indium intermixture, and these covering materials extending onto the steps and feathering out from them. A height comparison of Cu_3In with respect to the Cu_2In alloy is therefore not possible.

6. Conclusions

We have observed the formation of two surface alloys by deposition of indium on Cu(111): Cu_2In and Cu_3In. Indium enters the Cu(111) surface substitutionally, and with more indium deposition there is copper–indium interdiffusion in the first few layers. This causes about 15% copper lattice expansion. Indium seems to prefer to be surrounded by copper, as is seen in both alloy structures (figure 8) and seems to trap other indiums weakly in the second-neighbour position [4–9]. The difference of atomic radii of the two system components favours the creation of surface alloys with a surplus of copper because indium's larger size forces exchanges between atoms that will lead to a smaller lattice expansion. Although indium is much larger, this large atomic size mismatch does not impede surface alloy formation, either in the case studied here or in the case of antimony on copper or silver.

There is no obvious path from Cu_2In to Cu_3In with increasing indium deposition. Rather, the data suggest that Cu_2In reaches its maximum coverage, and then more indium deposition favours diffusion of indium atoms into deeper layers (or equivalently, diffusion of copper up through the deposited indium). The morphology of Cu_2In as seen in the STM images (figure 6) suggests that it may be stabilized by vacancies and larger holes. The edges and holes in the Cu_2In agglomerates seem to be likely sites for transformation to Cu_3In. At higher coverages of indium, island growth at steps also appears, apparently caused by indium diffusion.

The whole picture of the growth and replacement of surface alloys in this system can be summarized as follows: with initial deposition of indium, Cu_2In begins to form in the surface layer, with approximately full coverage at 0.4–0.5 ML indium. Then, additional indium first piles up briefly while copper diffuses upwards to form Cu_3In. Cu_3In forms in the first several layers, and only with the addition of more than 3–4 ML indium is a pure indium surface coverage achieved.

Acknowledgments

The authors acknowledge the support of a German–Polish 'Bilateral Cooperation in Science and Technology' grant (POL-98-039) from the Bundesministerium für Bildung und Forschung, as well as support from the Deutsche Forschungsgemeinschaft (SFB 513), the German–American Fulbright Commission (WEE) and the Department of Physics and Astronomy, Brigham Young University (WEE).

References

[1] Keppner W, Klas T, Körner W, Wesche R and Schatz G 1985 *Phys. Rev. Lett.* **54** 2371
[2] Albrecht M, Maier A, Treubel F, Maret M, Poinsot R and Schatz G 2001 *Europhys. Lett.* **56** 884
[3] van der Vegt H A, Alvarez J, Torrelles X, Ferrer S and Vlieg E 1995 *Phys. Rev.* B **52** 17443
[4] Klas T, Fink R, Krausch G, Platzer R, Voigt J, Wesche R and Schatz G 1989 *Surf. Sci.* **216** 270
[5] van Siclen C DeW 1995 *Phys. Rev.* B **51** 7796
[6] Breeman M, Barkema G T and Boerma D O 1994 *Phys. Rev.* B **49** 4871
[7] Breeman M and Boerma D O 1992 *Phys. Rev.* B **46** 1703
[8] Breeman M, Dorenbos G and Boerma D O 1992 *Nucl. Instrum. Methods Phys. Res.* B **64** 64
[9] Breeman M and Boerma D O 1993 *Surf. Sci.* **287/288** 881
[10] Frenken J W M, van Gastel R, van Albada S B, Somfai E and van Saarloos W 2002 *Appl. Phys.* A **75** 11
[11] van Gastel R 2001 The atomic slide puzzle: vacancy-mediated diffusion of a surfactant *Dissertation* University of Leiden (online publication at http://lions1.leidenuniv.nl/sections/cm/ip/group/theses/gastel/thesis.pdf)
[12] Soares E A, Bittencourt C, Nascimento V B, de Carvalho V E, de Castilho C M C, McConville C F, de Carvalho A V and Woodruff D P 2000 *Phys. Rev.* B **61** 13983
[13] Aufray B, Giordano H and Seidman D N 2000 *Surf. Sci.* **447** 180
[14] de Vries S A, Huisman W J, Goedtkindt P, Zwanenburg M J, Bennett S L, Robinson I K and Vlieg E 1998 *Surf. Sci.* **414** 159
[15] Bailey P, Noakes T C Q and Woodruff D P 1999 *Surf. Sci.* **426** 358
[16] Meunier I, Gay J-M, Lapena L, Aufray B, Oughaddou H, Landemark E, Falkenberg G, Lottermoser L and Johnson R L 1999 *Surf. Sci.* **422** 42
[17] Woodruff D P and Robinson J 2000 *J. Phys.: Condens. Matter* **12** 7699
[18] Seah M P and Dench W A 1979 *Surf. Interface Anal.* **1** 2
[19] Klas T, Fink R, Krausch G, Platzer R, Voigt J, Wesche R and Schatz G 1988 *Europhys. Lett.* **7** 151
[20] Klas T 1987 Untersuchung einkristalliner Cu-Oberflächen mit ^{111}In-Hyperfeinsonden als mikroskopischen Beobachtern *Diplomarbeit* University of Konstanz
[21] Gimple V 1999 Untersuchungen zur Surfactant-Wirkung von indium beim Wachstum von Kobalt auf Kupfer(111) *Diplomarbeit* University of Konstanz
[22] Wider H 2002 Surfactant-Wirkung von indium auf das Wachstum von Kobalt auf der Kupfer(111)-Oberfläche *Dissertation* University of Konstanz (online publication at http://www.ub.uni-konstanz.de/kops/volltexte/2002/873)
[23] Hume-Rothery W 1931 *The Metallic State* (Oxford: Clarendon)